A new phase obtained by oxidation of nanosized spinel $MnFe_2O_4$

T. I. Lazarova, D. G. Kovacheva*

*Institute of General and Inorganic Chemistry, Bulgarian Academy of Sciences,
Acad. G. Bonchev str., Bl 11, 1113 Sofia, Bulgaria*

In a bulk form $MnFe_2O_4$ is a partially inverse spinel where about 80% of Mn^{2+} ions are located at tetrahedral (A) coordination sites. $MnFe_2O_4$ is used as catalyst, as adsorbent for removing heavy metals in water, as ferrofluids, in biomedicine, in energy storage devices and others. Solution combustion synthesis was used for the preparation of nanosized $MnFe_2O_4$ with a mixture of two fuels – glycine and glycerol (0.75:0.25 reducing power ratio). The resulting material was characterized by X-ray diffraction (XRD). As-prepared sample is single phase spinel with unit cell parameter 8.470 Å. After a thermal treatment in argon flow at 40 °C for 2 hours, the unit cell parameter increases to 8.488 Å. Additional thermal treatment at 400 °C in air resulted in a new diffraction pattern, indicative for structural transformation. Indexing the entire set of diffraction lines gave a solution with a good reliability factor within a rhombohedral space group (unit cell parameters a = 6 Å and c = 28.6 Å). Possible space groups were R3, R3m and R–3m. Preliminary structural data for the new phase are presented. The new structure is closely related to that of the spinel. It was found that the oxygen layer packing sequence remained unchanged, but the displacement of the oxygen positions resulted in lowering of the cubic symmetry to hexagonal. The arrangement of the cation positions also remains close to that of the spinel, alternating the Oh_3 layers and T_2O layers. The cation to anion ratio of the new phase is considered to be close to that of γ-Fe_2O_3 and is cation deficient.

Keywords: $MnFe_2O_4$, oxidation, rhombohedral spinel-like phase.

INTRODUCTION

The spinel ferrites, MFe_2O_4 (*M* = Co, Ni, Mn, Mg, etc.) are attractive for many technological applications due to their specific electrical and magnetic properties including high permeability and moderate magnetization [1]. These properties define their use in many devices like filters, phase shifters, circulators, high frequency transformers and other microwave applications. Recently, they were also applied successfully in biomedical technologies for cancer remediation therapies [2, 3]. Their importance in electronics stems in part from their applicability for efficient production of large quantities of clean materials at relatively low temperatures. It has been shown that the cation distribution in spinel ferrites determines their electrical, magnetic and catalytic properties [4]. Manganese ferrite $MnFe_2O_4$ is a well-known microwave ferrite material with a partially inverse spinel structure in a bulk form. Earlier work, which studied the size dependent magnetic properties of 5–15 nm $MnFe_2O_4$ particles, suggested that its Néel temperature T_N increased with decreasing particle size in a manner consistent with a finite size scaling model [5]. Some reports show that the cation distribution remained essentially the same in $MnFe_2O_4$ particles of different sizes and indeed the small particles have higher T_N than larger ones [6]. Single phase $MnFe_2O_4$ powders having crystallite sizes ranging between 9.5 and 40 nm have also been obtained by mechanochemical synthesis. The degree of inversion in these samples was found to remain unchanged and independent of size. The Néel temperature was constant irrespective of the particle size. [7] The cation distribution and oxidation state of ferrous and nonferrous ions are essential in understanding the magnetic and electronic properties of ferrite materials. The occupancy of Mn ions at octahedral sites was found to greatly influence the Néel temperature[8].

EXPERIMENTAL

Solution combustion synthesis was applied for the preparation of nanosized $MnFe_2O_4$ using a mix-

---

* To whom all correspondence should be sent:
E-mail: didka@svr.igic.bas.bg

ture of two types of fuel, namely glycine and glyce-rol in a 0.75:0.25 reducing power ratio. Starting reagents – analytical grade $Mn(NO_3)_2.4H_2O$ and $Fe(NO_3)_3.9H_2O$, were taken as oxidants and precursors in a molar ratio 1:2. The fuel to oxidant ratio (1:1) was calculated on the base of oxidation and reduction power of the corresponding compounds as proposed by Jain et al. [9]. The calculated amounts of all starting reagents were dissolved in deionized water and the resulting solution was heated on a plate with magnetic stirrer. Soon after the dehydration of the solution, it reaches its flash point and ignites releasing a large amount of heat resulting in a fine powder denoted as "as prepared" sample. Two samples were obtained – first by thermal treatment of the as prepared sample at 400 °C in argon atmosphere for 2 hours and the second – by subsequent thermal treatment of previous sample for 12 h at 400 °C in air.

The resulting materials were characterized by X-ray diffraction (XRD). Powder XRD patterns were registered at room temperature on a Bruker D8 Advance diffractometer with CuKα radiation and LynxEye detector. The Rietveld refinement procedure was performed with the Topas 4.2 program [10].The set of parameters that were refined include: zero shift, coefficients (7) of the background Chebyshev polynomials, the absorption correction coefficient, scale factor, unit cell parameters, positional parameters, occupancies and thermal displacement parameters of the ions presented in the structure. The peak shapes were described according to the fundamental parameters approach taking into account the geometry of the diffractometer and the optical devices on the beam path.
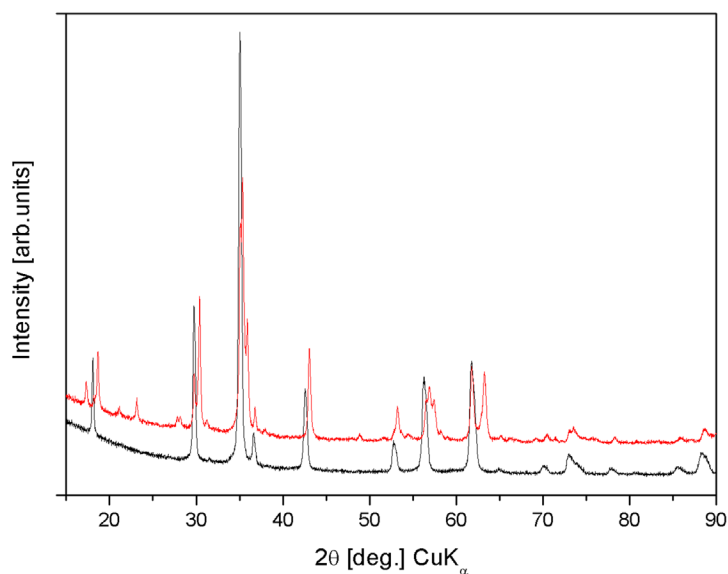
RESULTS AND DISCUSSIONS

The as-prepared sample is a single phase with spinel-type structure having unit cell parameter 8.470 Å and mean crystallite size of about 40 nm. After the thermal treatment in argon flow at 400 °C for 2 hours, the unit cell parameter increases to 8.488 Å and the average crystallite size decreases to 35 nm. Additional thermal treatment at 400 °C of the same sample in air resulted in a new diffraction pattern, indicative for structural transformation Fig. 1. The detailed analysis of the newly obtained diffraction pattern shows that the positions and intensities of its reflexions can not be unambiguously attributed to any known phases in the Mn-Fe-O system, neither as mixed or simple oxides.

Indexing the entire set of diffraction lines with Topas 4.2 delivered a solution with a good confidence factor within a rhombohedral space group with unit cell parameters (a = 6 Å and c = 28.6 Å). On the basis of systematic extinctions, possible space groups were R3, R3m and R–3m.

The axial metric relations showed that this unit cell has the following relationships with that of the spinel:

$$aH = aSp/\sqrt{2},$$
$$cH = 6aSp/\sqrt{3},$$

where aH and cH are the cell parameters of the rhombohedral cell in hexagonal representation and aSp is the cell parameter of the cubic spinel. Having in mind the cell relations mentioned above several models for the structure of the new phase were built. The models assuming hexagonal close packing of the oxygen atoms did not lead to plausible solutions

Fig. 1. Powder diffraction patterns of the samples of $MnFe_2O_4$ obtained after thermal treatment in argon (black) and in air (red).

thus models with cubic close packing were further considered. As a starting model for the crystal structure refinement the data for oxygen positions in cobaltian aerugite, $Co_{8.5}As_3O_{16}$ (65630-ICSD) were taken. The cation positions were further determined. The Rietveld refinement of the model structure showed that about 10 mass% of the sample is residual spinel. Preliminary structural data for the new phase are presented in the Table 1. Rietveld plot is presented in Fig 2. The polyhedral presentation of the structure is given in Fig 3.

The new structure is closely related to that of the spinel. It was found that the oxygen layer packing sequence remained unchanged (a cubic close packing), but the displacements of the oxygen positions resulted in disappearance of two of the trifold axes.

As a result the cubic symmetry decreases to hexagonal. The arrangement of the cation positions also remains close to that of the spinel, alternating Oh3 and T2O layers. Due to the supposed oxidation of the cations, the cation to anion ratio of the new phase should be close to that of the γ-Fe_2O_3 (maghemite) and is assumed to be cation deficient. Unlike maghemite, where cation vacancies are distributed with preserving the cubic symmetry, in the current structure the vacancies seem to be located in one position (the octahedral position in one of the T2O layers) which is in good agreement with the conclusions made by other authors [11]. Due to the small difference in atomic scattering factors between iron and manganese ions in the presented preliminary structure refinement the cations are distributed over
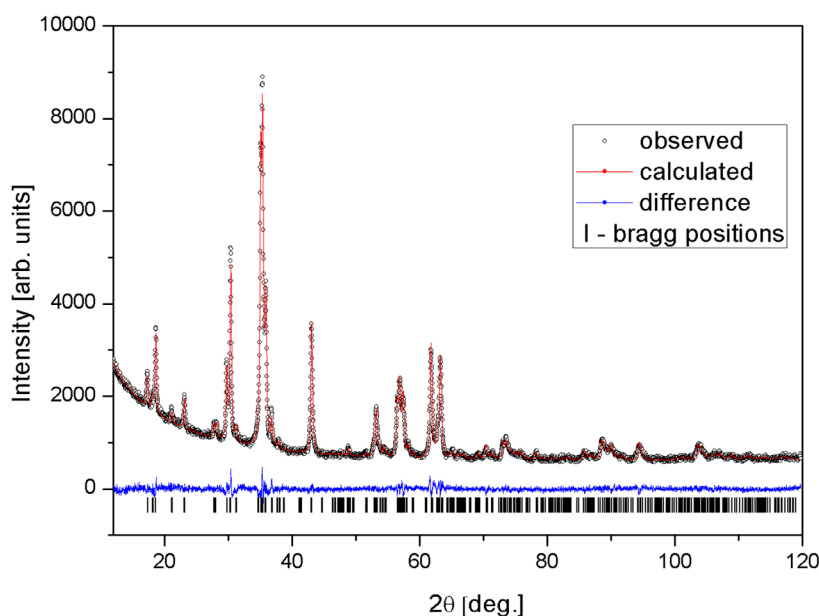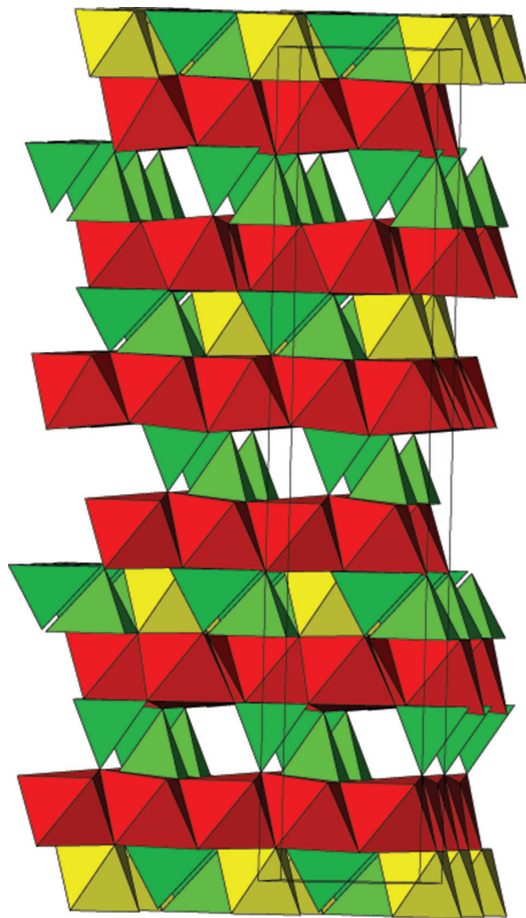

Fig. 2. Rietveld plot of the oxidized MnFe₂O₄.

Table 1. Preliminary structural data for the new phase
S.G. R–3m, Unit cell parameters: *a* (Å) = 6.0060(2), *c* (Å)=28.529(1)
Rbragg – 1.05, Rwp – 3.92, GOF – 1.265

Site	Multiplicity	Ion	x	y	z	Occupancy	B iso
O1	18	O–2	0.1447(6)	–0.1447(6)	–0.0438(3)	1	0.84(8)
O2	6	O–2	0	0	0.3784(5)	1	0.84(8)
O3	6	O–2	0	0	0.1256(6)	1	0.84(8)
O4	18	O–2	0.4974(7)	–0.4974(7)	–0.1190(3)	1	0.84(8)
Fe1	18	Fe+3	–0.1706(2)	0.1706(2)	0.9137(9)	1	1.01(4)
Fe2	3	Fe+3	0	0	0	1	1.01(4)
Mn1	6	Mn+3	0	0	0.8096(2)	1	0.45(4)
Mn2	6	Mn+3	1/3	–1/3	–0.0222(1)	1	0.45(4)

will be refined on the basis of additional experiments including Mössbauer spectroscopy and neutron diffraction.

Fig. 3. Polyhedral presentation of the structure of the new phase – red octahedra Fe1, yellow octahedra – Fe2, green tetrahedra – Mn1 and Mn2.

the tetrahedral and octahedral positions according to the distribution usually found in the spinel phase. The actual cation oxidation states and distribution

REFERENCES

1. J. Smith, J. Wijn, Ferrites, Cleaver-Hume, London, 1959.
2. L. Bauer, S. Situ, M. Griswold, A. Samia, *Nanoscale*, **8**, 12162 (2016).
3. Y. Peng, Z. Wang, W. Liu, H. Zhang, W. Zuo, H. Tang, *Dalt. Trans.*, **44**, 12871 (2015).
4. V. Tyrpekl, J. Vejpravova, A. Roca, N. Murafa, L. Szatmary, D. Niznansky, *Appl. Surf. Sci.*, **257**, 4844 (2011).
5. P. Chen, C. Sorenson, K. Klabunde, G. Hadjipanayis, E. Devlin, A. Kostikas, *Phys. Rev. B*, **54**, 9288 (1996).
6. C. N. Chinnasamy, A. Narayanasamy, N. Ponpandian, R. J. Josephus, B. Jeyadevan, K. Tohji, and K. Chattopadhyay, *J. Magn. Magn. Mater.*, **238**, 281 (2002).
7. G. Kulkarni, K. Kannan, T. Arunarkavalli, C. N. R. Rao, *Phys. Rev. B*, **49**, 724 (1994).
8. C. N. Chinnasamy, A. Yang, S. D. Yoon, K. Hsu, M. D. Shultz, E. E. Carpenter, S. Mukerjee, C. Vittoria, V. G. Harris, *J. Appl. Phys.*, **101**, 09M509 (2007).
9. S. Jain, K. Adiga, V Pai Verenekar, *Combust. Flame*, **40**, 71 (1981).
10. TOPAS V4: General profile and structure analysis software for powder diffraction data, User's Manual, Bruker AXS, Karlsruhe, Germany Bruker AXS, 2008.
11. P. Tailhades, A. Rousset, R. Bernaoud, A. Fert, B. Gillot, *Mat. Chem. Phys.*, **17**, 521 (1987).